

## On the occurrence of non-reflecting cross-shore profiles along Estonian coasts of the Baltic Sea

Ira Didenkulova<sup>a</sup>, Tarmo Soomere<sup>a,b</sup>, Katri Pindsoo<sup>a</sup> and Sten Suuroja<sup>c</sup>

<sup>a</sup> Institute of Cybernetics at Tallinn University of Technology, Akadeemia tee 21, 12618 Tallinn, Estonia; ira@cs.ioc.ee

<sup>b</sup> Estonian Academy of Sciences, Kohtu 6, 10130 Tallinn, Estonia

<sup>c</sup> Geological Survey of Estonia, Kadaka tee 82, 12618 Tallinn, Estonia

Received 29 April 2013, in revised form 27 May 2013

**Abstract.** Cross-shore beach profiles along Estonian coasts of the Baltic Sea are analysed from the viewpoint of the frequency of occurrence of convex sections that may support non-reflecting wave propagation and unexpectedly high run-up events. In total 194 beach profiles, measured in 2006–2011 at 16 locations, are examined by means of their approximation with the power function  $h(x) = Ax^b$ . About half of the profiles can be adequately approximated using a single power function. These profiles are almost all concave. The relevant exponents are clustered around  $b = 2/3$  that is characteristic to the Dean's Equilibrium Profile. The rest of the profiles can be divided into two sections, each of which is approximated by a power function. The underwater sections of such profiles predominantly match the Dean's Equilibrium Profile. About 10% of the subaerial sections (about 7% of all examples) have the exponent close to  $b = 4/3$ , for which high run-up events are likely.

**Key words:** beach profile, wave run-up, marine coastal hazards, Dean's Equilibrium Profile, Estonia, Baltic Sea.

### 1. INTRODUCTION

Wave dynamics in the coastal zone has major implications not only for the design and construction of various coastal engineering structures but also for the safety of users of the nearshore and the coast. It is well known that specific wave phenomena such as tsunamis [<sup>1,2</sup>] may lead to large-scale devastation. Storm surges can provide an equally or even larger danger to low-lying areas [<sup>3,4</sup>]. Rough storm waves may cause substantial deterioration of natural coasts [<sup>5</sup>] and severely harm various structures in the vicinity of the waterline and in inundated areas [<sup>6</sup>]. The impact of single large-amplitude waves in the nearshore and

especially the danger associated with their possible run-up along gently sloping beaches is frequently ignored in the coastal hazard assessment [7]. The research into such waves and the related danger, stemming from their run-up, are classical topics of the ocean and coastal engineering [8-10]. They have been mostly applied to tsunami studies [10-12] and to a lesser extent to studies of local processes such as overtopping [13].

The problem of possible high run-up becomes increasingly important in the light of evidence of unexpectedly high waves that at times appear in the immediate vicinity of the waterline. This phenomenon is known under different names in different communities. In the USA it is frequently called “squall line wave” [14] whereas in the German-speaking community they are known as “seebär” and on the coasts of Sweden as “sjösprång.” Such waves are frequently associated with meteorological tsunamis [15] or the phenomenon called “rissaga” [16]. In many occasions their characteristic period considerably differs from that of meteotsunamis and they resemble freak or rogue waves [17]. Such waves often pass unseen in the open ocean but they may cause considerable damage in the nearshore [18-19]. This damage is typically minor to coastal structures and in terms of beach erosion as the duration of the impact is shorter and associated forces are usually smaller than those stemming from storm waves. The prime dangers are their sudden appearance and the impact to users of the coastal zone through their ability to penetrate far inland and to exert unexpectedly high run-up.

The potential of the penetration of a wave into inland (wave run-up height) has been a subject of intense studies [20]. The run-up height depends not only on the wave height and period but also on whether the wave is a part of a wave group [9], a solitary wave or an  $N$ -wave [10], or whether it has an asymmetric initial profile [21]. The associated danger also strongly depends on the bathymetry of the nearshore region and the run-up domain [20] that may cause wave focusing and amplification [22,23] or may lead to dissipation of wave energy.

In several cases the classical theory has not properly predicted or explained the unusually high run-up of otherwise well-documented tsunamis. For example, the 17 July 2006 Java tsunami [24], the 2009 American Samoa tsunami and the 2011 Tohoku tsunami penetrated much farther inland than it has been predicted by the theory of wave propagation along a plane beach [25].

A possible reason for the discrepancy is that numerical models and early-warning systems often use a constant-slope beach approximation for the prediction of wave run-up. This simplification may lead to underestimation of wave-induced hazards for (non-reflecting) coastal profiles of specific type. For example, propagation of long waves over certain convex profiles is not accompanied by wave energy reflection [26]. This phenomenon occurs when the water depth  $h$  increases as  $h(x) \sim x^{4/3}$  or as  $h \sim x^4$  (so-called quartic profile [27]) with the distance  $x$  from the waterline [28]. Although non-reflecting propagation is evidently not able to concentrate the entire wave energy into the vicinity of the waterline, unexpectedly large amounts of water may reach much higher grounds in such situations than along partially reflecting beach profiles.

The properties of wave transformation and impact (e.g., in terms of breaking, run-up or set-up) along the classical Dean's Equilibrium Profile with  $h(x) \sim x^{2/3}$  and similar concave profiles are relatively well known. Convex profiles infrequently occur on natural beaches and much less attention has been paid to wave propagation along these profiles [29]. While the formation of quartic profiles is not likely along sedimentary coasts, non-reflecting beach profiles with  $h(x) \sim x^{4/3}$  may exist in natural conditions. Such profiles have been shown to regularly occur and to remain stable for a longer interval (Fig. 1) under the joint effect of short-period windseas and transient groups of long vessel waves [30]. Similar properties of natural wave systems may often occur in semi-sheltered domains with highly intermittent wave climate containing more or less equal energy of short, locally generated wind waves and long, remotely generated swells.

The described features raise the question about the potential of naturally occurring convex profiles. The adjacent subaerial regions may be intrinsically associated with an increased level of marine coastal hazards. The purpose of this paper is to quantify, to a first approximation, the potential of this type of coastal hazard for Estonian coasts. It is not likely to occur along long sedimentary coastal stretches that are open to the predominant wave approach directions and where a concave equilibrium profile is usually present [14,31]. It may be much more frequent along fragmented coasts that consist of relatively short sections of sedimentary stretches of highly variable exposure to wind waves. These stretches (especially in the Gulf of Finland) often host a combination of wave climate from local waves and remote swells. Moreover, many coasts of Estonia are not sedimentary and represent basically random shapes of limestone or sandstone scarps. As the focus is on the establishing whether this kind of coastal hazard could be present at all based on the pool of measured coastal profiles, we intentionally ignore the geological and geographical setting (e.g. the grain size or the approach direction of the predominant waves) along the particular coastal

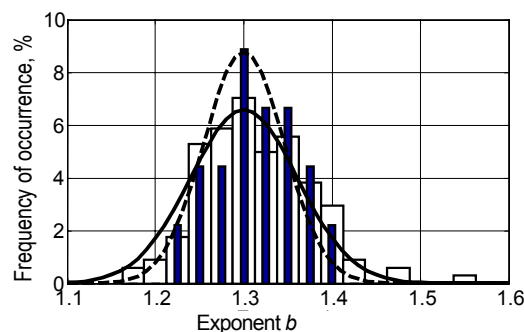


**Fig. 1.** Distribution of the exponent  $b$  in the power law approximation  $h \sim x^b$  for all measured beach profiles (white bars) and for early morning profiles (filled bars) at Pikakari Beach (Tallinn Bay, Baltic Sea) on 12 June–1 July 2009. Solid and dashed lines correspond to the approximations of the empirical distributions by the corresponding normal distributions [30].

stretches. For the same reason we intentionally ignore the seasonal variation of the profiles. We admit that this approach is only able to provide an estimate of the formal probability of occurrence of such profiles and sheds no light on where or when exactly they may occur.

## 2. POWER FUNCTION APPROXIMATION OF COASTAL PROFILES

There exist many ways to approximate the shape of coastal profiles. The simplest one is to assume that the nearshore seabed is a sloping plane. Although not exactly realistic, it is still widely used in various wave studies and often leads to very reasonable results [32,33]. The natural coastal profiles on sedimentary beaches tend to have a universal shape [34]. Their most frequently occurring appearance from the waterline to the depth of closure can be adequately described using a power function

$$h(x) = Ax^b \quad (1)$$

for the increase in the water depth  $h$  with the distance  $x$  from the waterline. Here  $A$  is a certain coefficient, characterizing the properties of sediments [14,31]. For our purposes the values of the parameter  $A$  are immaterial and are not considered in what follows. Concave profiles correspond to  $b < 1$  while those with  $b > 1$  are convex and  $b = 1$  characterizes an inclined plane. The search for an equilibrium shape (eventually reached only as a long-term average) was initially based on empirical data [31,35]. The assumption of the uniform volumetric wave energy dissipation in the surf zone leads to the power law  $h = Ax^{2/3}$  [31] of the commonly used Dean's Equilibrium Profile. The exponent  $b$  may vary for different coastal areas. For Dutch dune profiles  $b = 0.78$  provides a better fit [36], and  $b$  varies from 0.73 to 1.1 for Israeli beaches [37]. Subaerial parts of sedimentary beaches (that are occasionally impacted by large waves during high water level) may exhibit even larger variability. For example, for such a beach near the waterline on the Island of Aegna (Tallinn Bay, Baltic Sea) the exponent  $b$  varied in the range 0.67–1.2 within only one relatively calm month [38].

Equation (1) seems to be applicable even in the most extreme conditions [39,40]. Various asymptotic approximations for beach profiles in terms of power laws are also used in theoretical models [37,41]. Other approximations of the beach profile (for example, exponential and logarithmic) [39,42] can be described by Eq. (1) in the vicinity of the waterline.

A beach profile may contain several sections with different values of  $A$  and  $b$  [43,44] and even both concave (usually close to the shoreline) and convex sections (usually further offshore where the equilibrium beach profile ends and the bottom slope increases). Such situations often occur in macrotidal environments that host substantial wave loads [45] and where the wave climate can be interpreted as a limiting case of bimodal wave systems where the periods of long (tidal or seiche) waves exceed those of wind waves by several orders of magnitude.

The properties of coastal profiles in Estonia are more complicated because of the highly variable geological setting of its coasts. Estonia is located between the Fennoscandian Shield and the East European platform (Fig. 2). While some sections of its about 3800 km long shoreline (e.g., the eastern coast of the Gulf of Riga) are sedimentary and relatively straight, it mostly has quite complicated geometry and geology [46]. Especially the coasts of the Gulf of Finland and of some islands of the West Estonian archipelago are fragmented into numerous peninsulas and bays deeply cut into the mainland [47]. These coasts are often dominated by limestone or sandstone formations or are protected from the wave impact by cobbles, pebbles and boulders.

The northern and north-western parts of Estonia are influenced by the neotectonic uplift whereas the south-western part of the coastline experiences slight subsidence. The dominant process is straightening of the coastline: erosion from the headlands and accumulation at bayheads. The Baltic Klint escarpment of Cambrian–Ordovician bedrock favours the formation of cliffs and scarps, part of which are found also under water in the nearshore. In northern Estonia there is a contact between harder Ordovician limestones and softer terrigenous rocks (that are prone to erosion) almost at the waterline. Harder rift limestones of Jaagarahu

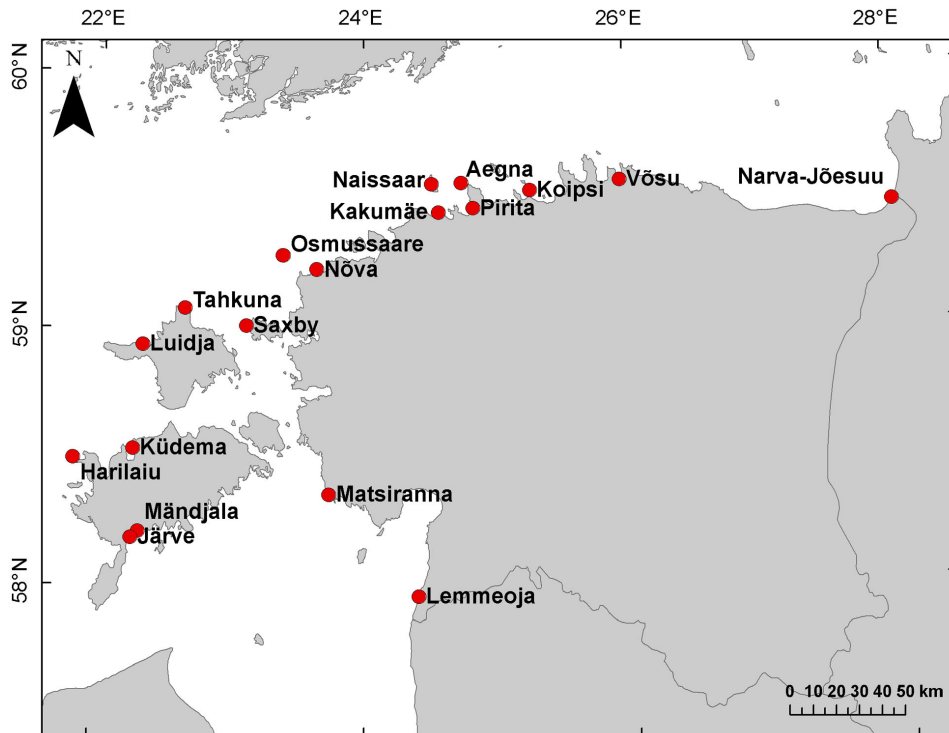


**Fig. 2.** Locations of regular measurements of cross-shore profiles along Estonian coasts in the framework of state monitoring program of beaches.

Stages and softer marls of Jaani Stage prevail in the north-western part of the Island of Saaremaa. It is thus natural that the relatively young, mainly rapidly developing and often non-equilibrium shores of Estonia are characterized by an extensive variation of coastal types [46]. As a result, the cross-shore profiles are also very different and do not always follow the classical profiles of sedimentary beaches.

We concentrate on the variety of beach profile shapes in terms of the occurrence of different values of the exponent  $b$  in the power law approximation (1) along Estonian coasts. This distribution is studied based on the profiling activities in the framework of the state monitoring program of beaches in 2004–2011 [48–52]. This data set represents the properties of coasts over several years (in most of cases 2004–2007) at several locations with very different wave loads and geological setting. The data set used in this paper contains 194 profiles from 16 sites located in widely open bays and beaches that are exposed to the predominant wave propagation directions. These locations are more or less homogeneously distributed along the Estonian coast (Fig. 2). This data set is also homogeneous in the sense that the profiling was performed using the same routine during the entire programme and at all locations.

### 3. VARIABILITY OF ESTONIAN COASTAL PROFILES

We focus on the nearshore parts of coastal profiles that may contribute to the formation of abnormal wave run-up. On the one hand, the relevant theory [27–29] requires waves to be long. This means that unexpectedly high run-up is formed in the nearshore where the water depth is well below 1/20 of the wavelength. Storm waves in the Baltic Sea have periods normally not exceeding 7–8 s [53] and are often accompanied by a substantial increase in the local water level. Therefore, the parts of the profile that are located deeper than about 2 m under mean water level are not likely to contribute to the dangerous run-up events. For this reason we discard the deeper parts of the profiles. On the other hand, it is likely that a part of the normally subaerial beach profile is flooded during a storm and contributes to the formation of unexpected run-up events. For this reason it is natural to include into the analysis subaerial profiles up to about 2–3 m above the mean water level.

The profiles in question have very different appearance (Fig. 3), from the one matching the Dean's Equilibrium Profile to shapes that reflect the presence of very stable, probably sandstone features. Consistently with the above-discussed worldwide variability of coastal profiles, some measured profiles can be adequately described using a single approximation  $h(x) = Ax^b$  over the entire profile (e.g., Kakumäe, profile 1 or Harilaid, profile 2 in Fig. 3), while other cross-sections exhibit two or more sections with clearly different properties. The profiles were separated into two subsets based on the correlation coefficient between the curve, corresponding to the best fit of parameters  $A$  and  $b$  in Eq. (1),

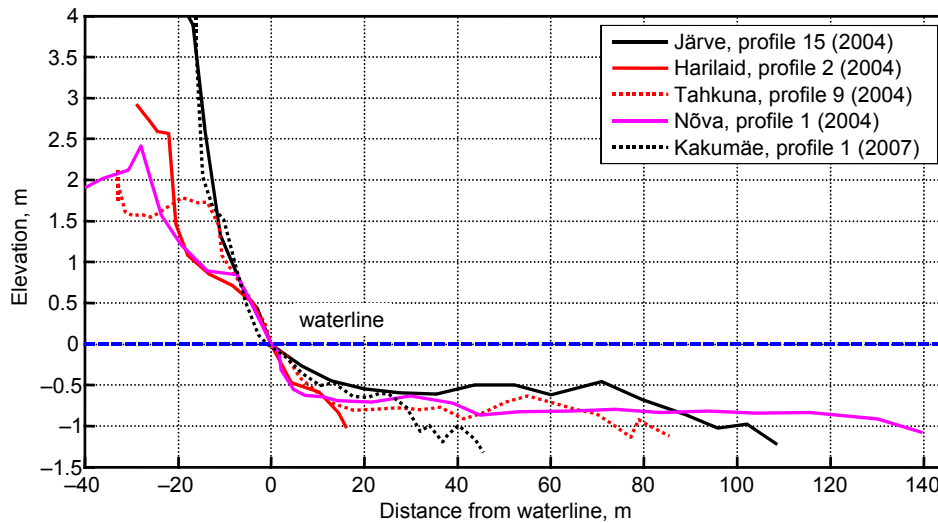


**Fig. 3.** A selection of single-section (Kakumäe, Harilaid) and two-section (Järve, Tahkuna, Nõva) beach profiles.

and the measured profile. A profile was approximated with a single power function (and called single-section profile below) if this coefficient was at least 0.87 (82 profiles out of 194) and was considered as consisting of two separate sections (and called two-section profile, 112 profiles) in the opposite case.

The separation point of the two-section beach profile into a seaward and a landward section was usually set at the middle of such profiles. Only profiles that had clearly separable concave and convex parts were divided at the inflection point. The resulting sections are interpreted as independent profiles called underwater and subaerial section, respectively. Doing so is consistent with the potential impact of water level variations on the wave propagation: the upper part of such a profile governs wave transformation and run-up during higher water levels whereas the lower part is responsible for wave propagation during lower water levels. The curved sections of 13 profiles are separated by long, practically even and horizontal, stretches of seabed. As such plain stretches may simply represent missing data, they are ignored in fitting the profiles with a power law.

The total set of 306 profiles (or profile sections) comes from only 16 sites, each of which is also represented by underwater and aerial sections. Although the time interval of surveys at individual locations was at least several months, profiles measured at the same location in different years are not completely independent as the beach profiles tend to keep a site-specific shape. Therefore, some profiles may form small clusters of highly correlated entries. The correlation is apparently relatively strong for single-section profiles and for the underwater sections of two-section profiles. The above-discussed extensive variability of the exponent  $b$  of a subaerial coastal profile over just one month [38] suggests that the correlation between subaerial sections, measured in different years, is

quite limited. This correlation evidently affects the resulting estimate of the probability of having favourable conditions for high run-up, compared to an ideally distributed data set, but probably will not change the basic conclusions of the analysis.

The values of the parameter  $b$  for single-section profiles vary significantly, in the range 0.2–1.64 (Fig. 4). The average value  $\bar{b} = 0.62$  (standard deviation  $\sigma_b = 0.24$ ) is, as expected, very close to  $b = 2/3$  for the Dean's Equilibrium Profile [31] and a large part of the values of  $b$  are clustered around  $b = 2/3$ . Although the majority of such profiles are characterized by  $b < 1$ , this set contains four convex beach profiles whereas in two cases  $b \cong 4/3$ . This feature suggests that the presence of convex beaches with specific wave-guiding properties [28] is possible even among beaches that can be approximated well by a single power function. Interestingly, no plane beach with  $b = 1$  exists among single-section profiles. This feature suggests that the model of plane beach (that is massively used in most of studies of wave propagation and run-up) is even less realistic than the model corresponding to  $b \cong 4/3$ .

The set of two-section coastal profiles contains 112 occasions and thus 224 individual sections. The average value of the parameter  $b$  for the underwater sections is 0.72 ( $\sigma_b = 0.56$ ) and thus also close to the characteristic value of the Dean's Equilibrium Profile. The overall shape of the distribution of the parameter  $b$  for these sections (Fig. 5) is similar to the distribution in Fig. 4 but its peak is located at values slightly smaller than  $2/3$  (Fig. 5). There are 17 cases where  $b > 1$ , including a few profiles with  $b \cong 4/3$  and two outliers with  $b > 2$ .

The subset of subaerial sections, however, has different properties. The distribution of exponents  $b$  is wider and centred around larger values of  $b$  than the one for single-section coasts. The average  $\bar{b} = 1.1$  and standard deviation  $\sigma_b = 0.80$  of this parameter substantially exceed similar values for the single-section and underwater beaches. There exists a considerable number of almost plane profiles with  $b \cong 1$ . Importantly, the frequency of occurrence of subaerial sections with  $b \cong 4/3$  is quite large, more than 10% (Fig. 5). As mentioned above, subaerial sections are frequently flooded during a storm and thus often

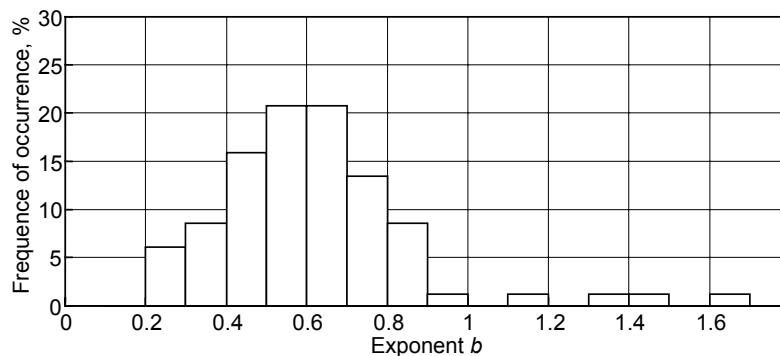
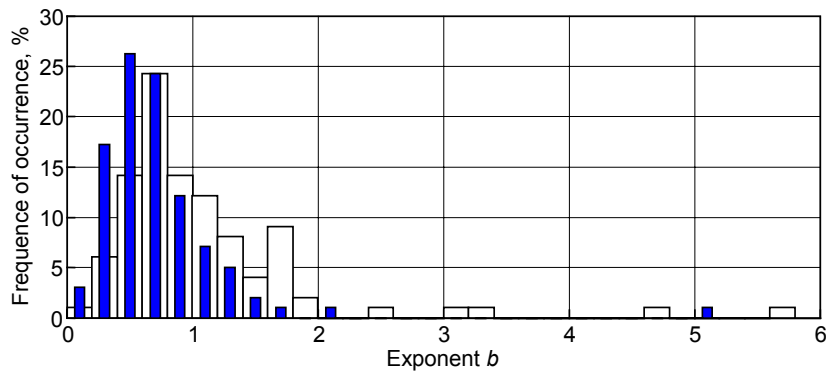


Fig. 4. Distribution of the exponent  $b$  for single-section beaches.



**Fig. 5.** Distribution of the exponent  $b$  for subaerial (white bars) and underwater (blue bars) sections of two-section profiles.

govern the transformation and run-up of the largest storm waves. The majority of subaerial sections still have  $b < 1$  and a substantial number of them matches the Dean's Equilibrium Profile. This feature suggests that subaerial sections are often shaped by waves that bring them in many occasions close to an equilibrium shape.

The maximum values reach  $b = 5.0$  for the underwater sections and  $b = 5.6$  for the subaerial parts. Such large values of  $b$  are not unique (e.g. cross-shore profiles for coasts of Guadeloupe have values around  $b = 4$  [<sup>54</sup>]) and evidently represent either underwater scarps or foets of coastal cliffs near the waterline. The evolution of such profiles is governed by local geological features rather than by wave activity. Their presence suggests that even quartic profiles may occur in the Estonian coastal zone.

The distribution of all values of the parameter  $b$  has a clearly defined maximum (represented in Fig. 6 by the range [0.6, 0.8]) at  $b = 2/3$ . Consistently

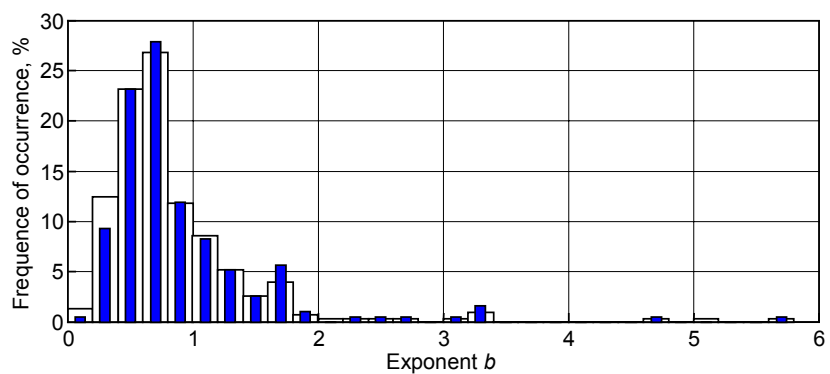


**Fig. 6.** Distribution of the exponent  $b$  for subaerial sections (narrow blue bars) and for all profiles (wide white bars).

with the above, considerable amount of virtually plane slopes occurs in the Estonian coastal waters. More importantly, a substantial number of the entire beach profiles or their single sections have a shape of a power function with the exponent  $b \cong 4/3$ . The empirical probability for this exponent to fall into the range of [1.2, 1.6] is about 7%.

#### 4. DISCUSSION

The presented analysis first reflects several facts that are well known in the coastal research community for a long time, for example, that the majority of cross-sections of sedimentary coasts match the appearance of the classical Dean's Equilibrium Profile. It also demonstrates an extensive variability of the coastal profiles at different locations of Estonia in terms of the exponent  $b$  of the classical power function approximation for the water depth  $h(x) = Ax^b$ . The exponent varies from almost zero (horizontal seabed or subaerial beach) up to values 5–6 (that usually characterize very steep rocky coasts). The majority of the exponents are clustered around  $b = 2/3$  that corresponds to a uniform rate of wave energy loss per unit of water volume. In total, in about 60% of the cases this exponent is in the range from 0.4 to 1.0. Therefore, the use of this shape of coastal profiles for various estimates of sediment transport or loss [<sup>55,56</sup>] is generally justified in the Estonian nearshore. The frequently occurring values in the range of 0.2–0.4 suggest that situations, in which the assumption of a uniform wave energy loss per unit of water surface (equivalently, per unit of length of the coastal profile) that results in  $b = 2/5$ , are also frequent in this nearshore.

The analysis revealed an interesting relationship between the overall shape of a coastal profile and the exponent in the power function approximation. Namely, for the subset of profiles that approximately follow a single power law, the exponent is mostly  $b < 1$  and the profiles usually match the Dean's Equilibrium Profile. Although some convex profiles occur, this subset does not contain any profiles with a constant slope.

The situation is substantially different if a coastal profile cannot be adequately approximated by a single power function. In such cases its underwater part often matches the Dean's Equilibrium Profile with  $b = 2/3$ . Therefore, in low water conditions (e.g. on the coasts of the Gulf of Finland during easterly storms) the formation of non-reflecting coastal profiles with  $b \cong 4/3$  (that support unexpectedly high run-up) is also unlikely.

The upper (partially subaerial) sections of such coastal profiles, however, often exhibit different properties. Although many such sections also match the Dean's Equilibrium Profile, they are often convex. Several cases with  $b > 2$  apparently correspond to either cliffed coasts or to the presence of a coastal scarp near the waterline. Importantly, this exponent quite frequently approximately matches the value  $b \cong 4/3$  that is characteristic to non-reflecting profiles. Wave propagation along such beaches may lead to extreme wave amplification and

unexpectedly high run-up events [21]. In other words, sneaker-wave-like events may be uncommonly frequent and strong at such locations.

The key conclusion of the presented analysis is that conditions, favourable for unexpectedly high run-up, may occur with a significant probability, estimated here as about 7% for the set of Estonian coasts covered with the used data. Although the analysis is based on coastal profiles from 16 locations and profiles from a single location (albeit measured after long time intervals) are not independent, even this rough estimate suggests that the possibility of increased danger of wave attack is by no means negligible and should be accounted for in estimates of the exposure of people and their property to marine coastal hazards. The presented analysis suggests that this danger considerably depends on the water level. It is apparently very small in mean and low water level conditions but eventually increases rapidly when the water level increases and high waves arrive at higher sections of the coastal profile.

Finally, we stress that the method employed in this paper (especially the division of profiles with a relatively complicated shape into two sections) relies exclusively on statistical analysis of some parameters of the shape of coastal profiles and ignores the background geological setting. An implicit consequence of this approach is that the results only provide an estimate of the formal probability of occurrence of profiles that favour unexpectedly high run-up events but shed no light on where or when exactly they may occur. Therefore, the presented results are not directly applicable in coastal engineering and management and more detailed analysis (that includes the geological structure of different shore types, the presence of near-shore shoals and islands as well as predominant wave conditions that have shaped the coasts) is necessary for reliable estimates of the danger associated with high run-up.

## ACKNOWLEDGEMENTS

This study was a part of the project “Science-based forecast and quantification of risks to properly and timely react to hazards impacting Estonian mainland, air space, water bodies and coasts” (TERIKVANT) supported by the European Union (European Regional Development Fund, ERDF) and managed by the Estonian Research Council in the framework of the Environmental Technology R&D Programme KESTA. The research was partially supported by the targeted financing by the Estonian Ministry of Education and Research (grant SF0140007s11), Estonian Science Foundation (grants 8870 and 9125) and through support of the ERDF to the Centre of Excellence in Non-linear Studies CENS. ID acknowledges the support provided by the Alexander von Humboldt Foundation.

## REFERENCES

1. Lay, Th., Kanamori, H., Ammon, Ch. J., Nettles, M., Ward, S. N., Aster, R. C., Beck, S. L., Bilek, S. L., Brudzinski, M. R., Butler, Rh. et al. The Great Sumatra-Andaman Earthquake of 26 December 2004. *Science*, 2005, **308**, 1127–1133.
2. Mori, N., Takahashi, T., Yasuda, T. and Yanagisawa, H. Survey of 2011 Tohoku earthquake tsunami inundation and run-up. *Geophys. Res. Lett.*, 2011, **38**, L00G14.
3. Kim, K. O., Lee, H. S., Yamashita, T. and Choi, B. H. Wave and storm surge simulations for Hurricane Katrina using coupled process based models. *KSCE J. Civil Eng.*, 2008, **12**, 1–8.
4. Dube, S. K., Poullose, J. and Rao, A. D. Numerical simulation of storm surge associated with severe cyclonic storms in the Bay of Bengal during 2008–2011. *Mausam*, 2013, **64**, 193–202.
5. Orviku, K., Jaagus, J., Kont, A., Ratas, U. and Rivis, R. Increasing activity of coastal processes associated with climate change in Estonia. *J. Coast. Res.*, 2003, **19**, 364–375.
6. Lehrman, J. B., Higgins, C. and Cox, D. Performance of highway bridge girder anchorages under simulated hurricane wave induced loads. *J. Bridge Eng.*, 2012, **17**, 259–271.
7. Valdmann, A., Käär, A., Kelpšaitė, L., Kurennoy, D. and Soomere, T. Marine coastal hazards for the eastern coasts of the Baltic Sea. *Baltica*, 2008, **21**, 3–12.
8. Carrier, G. F. and Greenspan, H. P. Water waves of finite amplitude on a sloping beach. *J. Fluid Mech.*, 1958, **4**, 97–109.
9. Kobayashi, N. and Wurjanto, A. Irregular wave setup and run-up on beaches. *J. Waterw. Port Coast. Ocean Eng.*, 1992, **118**, 368–386.
10. Tadepalli, S. and Synolakis, C. E. The run-up of N-waves on sloping beaches. *Proc. Roy. Soc. Math. Phys. Sci.*, 1994, **445**, 99–112.
11. Titov, V. V. and Synolakis, C. E. Extreme inundation flows during the Hokkaido-Nansei-Oki tsunami. *Geophys. Res. Lett.*, 1997, **24**, 1315–1318.
12. Tadepalli, S. and Synolakis, C. E. Model for the leading waves of tsunamis. *Phys. Rev. Lett.*, 1996, **77**, 2141–2144.
13. Losada, I. J., Lara, J. L., Guanche, R. and Gonzalez-Ondina, J. M. Numerical analysis of wave overtopping of rubble mound breakwaters. *Coast. Eng.*, 2008, **55**, 47–62.
14. Dean, R. G. and Dalrymple, R. A. *Coastal Processes with Engineering Applications*. Cambridge University Press, Cambridge, 2002.
15. Monserrat, S., Vilibic, I. and Rabinovich, A. B. Meteotsunamis: atmospherically induced destructive ocean waves in the tsunami frequency band. *Nat. Hazards Earth Syst. Sci.*, 2006, **6**, 1035–1051.
16. Rabinovich, A. B. and Monserrat, S. Meteorological tsunamis near the Balearic and Kuril Islands: Descriptive and statistical analysis. *Nat. Hazards*, 1996, **13**, 55–90.
17. Kharif, C. and Pelinovsky, E. Physical mechanisms of the rogue wave phenomenon. *Eur. J. Mech. B Fluids*, 2003, **22**, 603–634.
18. Didenkulova, I. I., Slunyaev, A. V., Pelinovsky, E. N. and Kharif, Ch. Freak waves in 2005. *Nat. Hazards Earth Syst. Sci.*, 2006, **6**, 1007–1015.
19. Nikolkina, I. and Didenkulova, I. Rogue waves in 2006–2010. *Nat. Hazards Earth Syst. Sci.*, 2011, **11**, 2913–2924.
20. Levin, B. and Nosov, M. *Physics of Tsunamis*. Springer, Berlin, 2008.
21. Didenkulova, I. I., Zahibo, N., Kurkin, A. A., Levin, B. V., Pelinovsky, E. N. and Soomere, T. Runup of nonlinearly deformed waves on a coast. *Dokl. Earth Sci.*, 2006, **411**, 1241–1243.
22. Didenkulova, I. and Pelinovsky, E. Non-dispersive traveling waves in inclined shallow water channels. *Phys. Lett. A*, 2009, **373**, 3883–3887.
23. Didenkulova, I. and Pelinovsky, E. Runup of tsunami waves in U-shaped bays. *Pure Appl. Geophys.*, 2011, **168**, 1239–1249.
24. Fritz, H. M., Kongko, W., Moore, A., McAdoo, B., Goff, J., Harbitz, C., Uslu, B., Kalligeris, N., Suteja, D., Kalsum, K. et al. Extreme runup from the 17 July 2006 Java tsunami. *Geophys. Res. Lett.*, 2007, **34**, L12602.

25. Okal, E. A., Fritz, H. M., Synolakis, C. E., Borrero, J. C., Weiss, R., Lynett, P. J., Titov, V. V., Foteinis, S., Jaffe, B. E., Liu, P. L.-F. and Chan, I.-Ch. Field survey of the Samoa tsunami of 29 September 2009. *Seismol. Res. Lett.*, 2010, **81**, 577–591.
26. Clements, D. L. and Rogers, C. Analytic solution of the linearized shallow-water wave equations for certain continuous depth variations. *J. Aust. Math. Soc.*, B, 1975, **19**, 81–94.
27. Didenkulova, I. and Pelinovsky, E. Traveling water waves along a quartic bottom profile. *Proc. Estonian Acad. Sci.*, 2010, **59**, 166–171.
28. Didenkulova, I., Pelinovsky, E. and Soomere, T. Long surface wave dynamics along a convex bottom. *J. Geophys. Res.*, 2009, **114**, C07006.
29. Didenkulova, I. I. and Pelinovsky, E. N. Reflection of a long wave from an underwater slope. *Oceanology*, 2011, **51**, 568–573.
30. Didenkulova, I. and Soomere, T. Formation of two-section cross-shore profile under joint influence of random short waves and groups of long waves. *Marine Geol.*, 2011, **289**, 29–33.
31. Dean, R. G. Equilibrium beach profiles: characteristics and applications. *J. Coast. Res.*, 1991, **7**, 53–84.
32. Yeh, H., Liu, P. L.-F. and Synolakis, C. (eds). *Long-Wave Runup Models*. World Scientific, 1996.
33. Liu, P. L.-F., Yeh, H. and Synolakis, C. (eds). *Advances in Coastal and Ocean Engineering: Advanced Numerical Models for Simulating Tsunami Waves and Runup*. World Scientific, 2008.
34. Bruun, P. *Coast Erosion and the Development of Beach Profiles*. Beach Erosion Board Technical Memorandum No. 44, U.S. Army Engineer Waterways Experiment Station, Vicksburg, MS, 1954.
35. Dean, R. G. *Equilibrium Beach Profiles: U.S. Atlantic and Gulf Coasts*. Ocean Eng. Rep. 12, Dep. of Civil Eng., University of Delaware, Newark, 1977.
36. Steetzel, H. J. *Cross-shore Transport During Storm Surges*. Delft Hydraulics, Delft, The Netherlands, Publ. No. 476, 1993.
37. Kit, E. and Pelinovsky, E. Dynamical models for cross-shore transport and equilibrium bottom profiles. *J. Waterw. Port Coast. Ocean Eng.*, 1998, **124**, 138–146.
38. Didenkulova, I., Pelinovsky, E., Soomere, T. and Parnell, K. E. Beach profile change caused by vessel wakes and wind waves in Tallinn Bay, the Baltic Sea. *J. Coast. Res.*, 2011, Special Issue 64, 60–64.
39. Romańczyk, W., Boczar-Karakiewicz, B. and Bona, J. L. Extended equilibrium beach profiles. *Coast. Eng.*, 2005, **52**, 727–744.
40. Are, F. and Reimnitz, E. The *A* and *m* coefficients in the Bruun/Dean Equilibrium Profile equation seen from the Arctic. *J. Coast. Res.*, 2008, **24**, 243–249.
41. Kobayashi, N. Analytical solution for dune erosion by storms. *J. Waterw. Port Coast. Ocean Eng.*, 1987, **113**, 401–418.
42. Dai, Z.-J., Du, J.-Z., Li, C.-C. and Chen, Z.-S. The configuration of equilibrium beach profile in South China. *Geomorphology*, 2007, **86**, 441–454.
43. Inman, D. L., Elwany, M. H. S. and Jenkins, S. A. Shore-rise and bar-berm profiles on ocean beaches. *J. Geophys. Res.*, 1993, **98**, 18181–18199.
44. Bernabeu, A. M., Medina, R. and Vidal, C. A morphological model of the beach profile integrating wave and tidal influence. *Marine Geol.*, 2003, **197**, 95–116.
45. Wright, L. D. and Short, A. D. 1984. Morphodynamic variability of surf zones and beaches: A synthesis. *Marine Geol.*, 1984, **56**, 93–118.
46. Orviku, K. *Estonian Coasts*. Eesti NSV TA Geoloogia Instituut, Tallinn, 1974 (in Russian).
47. Orviku, K. and Granö, O. Contemporary coasts. In *Geology of the Gulf of Finland* (Raukas, A. and Hyvärinen, H., eds), 219–238. Valgus, Tallinn (in Russian).
48. Suuroja, S., Karimov, M., Talpas, A. and Suuroja, K. Mererannikute seire. Aruanne riikliku keskkonnaseire alamprogrammi “Mererannikute seire” täitmisest 2006. aastal. Tallinn, 2007.

49. Suuroja, S., Talpas, A. and Suuroja, K. Eesti Riikliku Keskkonnaseire mererannikute seire allprogrammi 2007. a aastaaruanne. Tallinn, 2008.
50. Suuroja, S., Talpas, A. and Suuroja, K. Eesti Riikliku Keskkonnaseire mererannikute seire allprogrammi 2008. a aastaaruanne. Tallinn, 2009.
51. Suuroja, S., Talpas, A. and Suuroja, K. Eesti Riikliku Keskkonnaseire mererannikute seire allprogrammi 2009. a aastaaruanne. Tallinn, 2010.
52. Suuroja, S., Talpas, A. and Suuroja, K. Eesti Riikliku Keskkonnaseire mererannikute seire allprogrammi 2010. a aastaaruanne. Tallinn, 2011.
53. Soomere, T. and Räämet, A. Spatial patterns of the wave climate in the Baltic Proper and the Gulf of Finland. *Oceanologia*, 2011, **53**(1-TI), 335–371.
54. Didenkulova, I., Nikolkina, I., Pelinovsky, E. and Zahibo, N. Tsunami waves generated by submarine landslides of variable volume: analytical solutions for a basin of variable depth. *Nat. Hazards Earth Syst. Sci.*, 2010, **10**, 2407–2419.
55. Kask, A., Soomere, T., Healy, T. R. and Delpeche, N. Rapid estimates of sediment loss for “almost equilibrium” beaches. *J. Coast. Res.*, 2009, **25**, Special Issue 56, 971–975.
56. Kartau, K., Soomere, T. and Tõnisson, H. Quantification of sediment loss from semi-sheltered beaches: a case study for Valgerand Beach, Pärnu Bay, the Baltic Sea. *J. Coast. Res.*, 2011, Special Issue 64, 100–104.

## **Mittepegeldavad rannaprofiilid Eesti rannikumeres**

Ira Didenkulova, Tarmo Soomere, Katri Pindsoo ja Sten Suuroja

Liiva- ja kliburandade rannaprofiilid on tavaliselt nõgusad ning veesügavust  $h$  neil kirjeldatakse adekvaatselt Deani tasakaalulise rannaprofiiliga  $h(x) = Ax^b$ , milles  $b = 2/3$ . Kumeratel rannaprofiilidel, mille puhul  $b = 4/3$  või  $b = 4$ , on võimalikud ootamatud kõrged lainerünnakud. Mererannikute seire raames aastail 2004–2011 16 kohas mõõdistatud 194 rannaprofiili alusel on analüüsitud taoliste lainerünnakute võimalust Eesti rannikul. Ligikaudu pooli (82) profiilidest kirjeldatakse adekvaatselt ühe astmefunktsiooniga. Need on peaaegu kõik nõgusad ja nende astmenäitajate  $b$  jaotuse maksimum on ligikaudu  $2/3$ . Ülejäänud profiilide veealuseid ja rannalähedasi osi käsitletakse omaette profiilidena. Veealused lõigud sarnanevad põhiosas Deani profiiliga. Veepiiri läheduses paiknevad ja osaliselt kuivale maale ulatuvad profiilid on aga sageli kumerad, kusjuures ligikaudu 10%-l juhtudest (7%-l kõigist profiilidest või nende osadest) on astmenäitaja  $b \cong 4/3$ . Seega on Eesti randades arvestatava sagedusega võimalikud ootamatud lainerünnakud.